Version of Record: https://www.sciencedirect.com/science/article/pii/S235294072400026X
Manuscript_39d735dd9d5d67459807505fe48adfd4

Flame-retardant cellulose-aerogel composite from agriculture waste for building insulation

Arpita Sarkar, Abdullah Islam, Long Zhu, Shenqiang Ren*

Department of Materials Science and Engineering, University of Maryland, College Park, MD 20742, USA

* Email: sren@umd.edu

Abstract: Bio-based thermal insulation materials are in high demand due to their availability, reproducibility, and carbon-sequestration nature. However, high flammability, moisture condensation, and high thermal conductivity of biogenic material are major concerns for sustainable building applications. In this study, we report the fire-retardant cellulose aerogel insulation nanocomposites derived from wheat straw and silica aerogel, in which sodium bicarbonate improves its fire retardancy. We combined blended straw fibers and hammermilled straw fibers to create a structural hierarchy composite. The blended straw, with its longer and thicker size, served as reinforcement, while the hammermilled straw fibers acted as filler. This hierarchical structure was further integrated with aerogel for applications in green buildings. The as-prepared materials show a low thermal conductivity of 24.1 mW/m.K, high flexural modulus of 736 MPa, hydrophobicity with a water contact angle of 110.42°, and excellent fire retardancy. Overall, this work provides an effective method for the synthesis of fire-retardant biogenic thermal insulation materials and shows a promising way for next-generation bio-based insulation materials.

Keywords: Biogenic materials, fire retardant cellulose-aerogel composites, thermal insulation.

Introduction

Recently, bio-based cellulose insulation materials derived from agriculture waste products are of great interest due to their sustainability, biocompatibility, low cost, and renewability [1-3]. Cellulose is considered the most abundant natural nontoxic biopolymer with huge carbon-storing potential and can be obtained from agricultural wastes like wheat straw, hemp fibers, and recycled pulp or paper [4-6]. Among them, wheat straw is considered a major eco-friendly natural source of cellulose because of its huge availability and lowest whole-life carbon emissions [7]. However, the major drawbacks of cellulose are its flammability, poor insulation, hygroscopic nature, and mechanical properties due to its inherent chemical structure [8, 9]. Especially cellulose is very easy to ignite without residual char formation which hinders its application in many fields including building insulation [10]. Therefore, improvement in the flame retardancy of cellulose base insulation materials along with good thermal and mechanical properties is a challenge of interest. Till now chemically modified organonitrogen, organophosphates, and halogenated organic compounds have been used as flame retardants in thermal insulation [11-14]. However, their harmful impact on human health and the environment restricts their use for future applications [15,16]. Therefore, the development of environmentally friendly, nontoxic, flame-retardant thermal insulation materials is necessary by employing green chemistry principles.

Here, we report the synthesis of cellulose-reinforced silica aerogel from wheat straw and silica aerogel. We have used sodium bicarbonate ($NaHCO_3$) as a flame retardant and developed a $NaHCO_3$-based silica aerogel which significantly improves the flame retardancy of the cellulose-aerogel nanocomposites. Moreover, sodium bicarbonate not only contributes to enhancing the flame-retardancy but also improves the microporosity of the resulting aerogel which offers excellent thermal insulation [17]. The as-prepared cellulose-aerogel nanocomposites display a very low thermal conductivity of 24.1 mW/m.K, good mechanical strength (flexural modulus of 736 MPa), recyclability of 90%, hydrophobicity with a water contact angle of 110.42^o, along with excellent flame retardancy. Overall, the as-synthesized flame-retardant nanocomposite coming from agriculture waste like wheat straw shows promising ways for the development of next-generation biogenic insulation materials.

Results and discussion

Chemical pretreatment is essential to extract cellulose and remove non-cellulosic parts (lignin and hemicellulose) from the wheat straw. In this regard, alkaline pretreatment has been proven to be very effective in removing lignin and hemicellulose from the wheat straw [18]. Figure 1a shows the schematic diagram of the alkaline pretreatment of straw fibers. Moreover, we have used alkaline-treated blended straw along with hammermilled straw for the fabrication of the composite to improve the thermal insulation and mechanical properties. Figure 1b shows the schematic of the synthesis of flame-retardant aerogel-cellulose composite using a new green chemistry approach. Sodium bicarbonate is an inexpensive and nontoxic material that begins to decompose into carbon dioxide, sodium carbonate, and water when heated to 60^{o}C, thus acts as a flame retardant and plays a key role in improving the fire retardancy of cellulose-aerogel nanocomposites [19, 20]. Figures 1c and S1 show the image of the as-prepared fire-retardant cellulose-aerogel composite.

Figure 2a shows the Fourier-transform infrared spectroscopy (FTIR) spectra of untreated and 0.5 M NaOH-treated blended and hammermilled straw fibers. The typical peaks of cellulose appeared in the region between 3313 and 2884 cm^{-1} due to the stretching vibration of O-H and

C-H respectively. The peak intensity has been significantly increased after sodium hydroxide pretreatment both in the case of blended and hammermilled straw which indicates that the pretreatment results in higher cellulose content than that of untreated straw [21]. Moreover, the peak for amorphous cellulose appeared at 894 cm^{-1} which also shows an increasing trend in the case of the pretreated fibers than the untreated straw. Figure 2b illustrates the thermogravimetric analyses (TGA) of the untreated and NaOH-treated straw fibers. All the samples degraded between 200 to 390ºC. At first, the small weight loss occurs around 100ºC due to the evaporation of moisture. The major weight loss appears between 240-390ºC due to cellulose degradation. The NaOH-treated wheat straw shows higher degradation temperature and higher stability than the untreated samples which indicates partial removal of lignin and hemicellulose. The morphology and structural change of the untreated and NaOH-treated straw fibers have been studied using scanning electron microscopy (SEM) and are shown in Figs. 2c-f. Figures 2c and 2d show the SEM images of untreated raw wheat straw and blended straw which show a rigid, intact, and ordered structure, while the NaOH-treated blended straw (Fig. 2e) and hammermilled straw (Fig. 2f) showed dispersed and loose fibers which indicate the disruption of the lignin-hemicellulose-cellulose network.

To improve the thermal conductivity and mechanical strength we have introduced sodium hydroxide-treated hammermilled straw with blended straw for the fabrication of the composites. Figure 3a shows the thermal conductivity and flexural modulus of blended: hammermilled (B: H) straw composites in different ratios. The thermal conductivity of only blended straw and hammermilled straw is 35.7 and 35.9 mW/m.K respectively which have been significantly reduced in the case of blended: hammermilled (B: H) straw composites from 38.2 mW/m.K to 34.1 mW/m.K due to the increased porosity (Fig. S2). The optimum thermal conductivity of 34.1

mW/m.K is found in the case of B: H (90:10) composites. Besides the thermal conductivity, the flexural modulus of the composites also shows a higher value (526 MPa-422 MPa) than the only blended straw (232 MPa) which signifies overall improvement of thermal conductivity and mechanical strength upon the addition of hammermilled straw into the blended straw composites. Figures 3b-f and Fig. S3 show the SEM images of different ratios of blended and hammermilled composites. The SEM images clearly reveal the presence of both blended and hammermilled straw in the composites. As the B: H (90:10) composite shows optimum thermal conductivity we have used the B: H (90:10) straw fibers for the fabrication of cellulose-aerogel composites.

Flame retardancy and thermal stability are of great importance for thermal insulation materials. To improve flame retardancy along with thermal insulation we have synthesized sodium bicarbonate containing TEOS-based silica aerogel for the fabrication of cellulose-aerogel composites. At first, we studied thermogravimetric analysis (TGA) which can help to understand the mechanisms of flame resistance of the materials. Figure 4a shows the TGA analysis of different wt % of cellulose-aerogel composites and without aerogel composites. The main decomposition peaks of cellulose aerogel composites become less intense and shift towards lower temperatures than the without aerogel composites, supporting that sodium bicarbonate is crucial for enhancing the flame retardancy of the composites [17, 22]. Figure 4b shows the thermal conductivity change with increasing different aerogel concentrations in the cellulose-aerogel composites. The thermal conductivity initially decreases from 29.6 to 24.1 mW/m.K with increasing the aerogel concentration from 10 to 30 wt % in the cellulose-aerogel composites. The optimum thermal conductivity of 24.1 mW/m.K is observed in the case of 30 wt % cellulose-aerogel composites due to the increased porosity (Fig. 4c) which is much better than other biogenic or mineral-based building materials (Table S1). However, the thermal conductivity shows an increasing trend above 30 wt % composites, which is unexcepted. We attributed this to the higher density and lower porosity of the samples with a higher concentration of aerogel. As shown in Figure 4b, the thermal conductivity is closely related to the density of the composite, with the addition of more aerogel than 30 wt % resulting in a higher composite density. Since the aerogel is not sintered, some organic residues from precursor during synthesis may still exist in the composite, adding mass to the high aerogel concentration samples. In Figure 4c, when the aerogel concentration is higher than 30 wt %, the porosity of the composite exhibits a decreasing trend. This decrease is primarily due to the aggregation of aerogel particles, contributing to enhanced thermal conductivity. Figure 4c displays the flexural modulus change with changing the aerogel concentration in the composites. The flexural modulus shows a decreasing trend from 680 to 640 MPa due to the increasing porosity with increasing aerogel concentration from 10 to 30 wt%. The flexural modulus increased from 640 to 736 MPa with a further increase in aerogel concentration above 30 wt% due to the increased density. The SEM images (Figs. 4d-f, Fig. S4) demonstrate that aerogel particles are embedded within the cellulose network, serving as reinforcement in the composite's performance. The composite contains mesoporous pores ranging from a few microns to tens of microns. Additionally, they distinctly illustrate the aggregation of aerogel particles as aerogel loading above 30 wt %.

Flame retardancy, water absorption capacity, and reusability are important criteria for thermal insulation materials. Figure 5a shows the wettability and the water absorption capacity of the wax-coated and uncoated cellulose-aerogel composite. The wax-coated composite shows 7 times lower water absorption capacity compared to that of the without-coated composite, which confirms the hydrophobic effect of the wax-coated gradient composite. Moreover, the water contact angle of the wax contact composite is 110.42^{o} (Fig. 5a inset) which also indicates the super hydrophobicity of the as-prepared composite. Figure 5b displays the SEM image of the wax-coated composite. Figure 5c shows the recyclability and reusability of the composite which shows a recovery percentage of 90 % and signifies the reusability and sustainability of the prepared cellulose-aerogel composite. Figs. 5d-f shows the flame retardancy of the without aerogel, TEOS aerogel composite, and sodium bicarbonate-containing TEOS aerogel-based composites. The without aerogel composites are ignited quickly and engulfed in flames within a few seconds while sodium bicarbonate containing TEOS aerogel composite composites exhibit a distinctly low burning rate which signifies that the sodium bicarbonate has significantly improves the fire retardancy of the composite (Video S1-S3). Sodium bicarbonate releases carbon dioxide and water vapor when exposed to heat. When a fire occurs, sodium bicarbonate decomposes at high temperatures, producing carbon dioxide gas. This gas helps dilute the oxygen in the vicinity of the fire, thereby reducing its availability and hindering the fire's ability to continue burning. Furthermore, the release of water vapor assists in cooling down the surrounding area, providing additional suppression against the fire.

Conclusion

We synthesized a fire-retardant cellulose aerogel composite from recycling agriculture waste and sodium bicarbonate containing TEOS-based aerogel. Sodium bicarbonate plays a key role in improving the thermal insulation as well as fire retardancy of the composite. The as-prepared cellulose-aerogel composite shows thermal conductivity of 24.1 mW m^{-1} K^{-1}, a flexural modulus of 736 MPa, hydrophobicity recyclability with a recovery of 90%, and excellent fire retardancy. The as-developed method can pave the way for the fabrication of green biobased insulation for building insulation.

Experimental Section

Materials: Tetraethyl orthosilicate (TEOS), mesitylene (1,3,5 trimethylbenzene; TMB), cetyltrimethylammonium bromide (CTAB), ammonium hydroxide, were purchased from Sigma-Aldrich. Wheat straw was purchased from Dumor Straw. Sodium hydroxide pellets (NaOH), and sodium bicarbonate were purchased from Fischer Scientific. The hydrophobic coating is carried out using wax purchased from U.C. Coatings.

Alkaline treatment wheat straw fiber

For alkaline treatment, at first, 20 gm of wheat straw fibers were blended into 500 ml of DI water. Next, the blended fibers were taken in a beaker and mixed with a solution of 0.5 M NaOH (% w/w) and stirred at 90^{o}C for a designated time of 2 hr. After that, the residue was filtered, washed with distilled water until the pH became neutral, and dried at 60 ^{o} C overnight. In a similar way, hammermilled wheat straws are mixed with 0.5 M NaOH solution and stirred at 90^{o}C for 2 hr. The cleaning and drying procedures are similar to the blended straw alkaline treatment.

Synthesis of TEOS aerogel precursor: The TEOS aerogel synthesis process is similar to our previous work with minor modifications [23]. Specifically, 18.75 gm of CTAB was dissolved in 1.5 lit of water at 35^{o}C and then 1.5 ml of ammonium hydroxide and 15 ml of mesitylene were added to it and stirred the solution for 4 hr. Then, 15 ml of tetraethyl orthosilicate (TEOS) was added slowly and the solution and left for stirring overnight at 35^{o}C. After that, sodium bicarbonate (10 gm) was added to the mixture and left for stirring for another 6 hr. After mixing the solution mixture was kept 60^{o}C oven for another 24 hours for gelation. The aerogel precursor was further dialyzed in 2.0 lit of DI water for purification and homogenized using a mechanical agitator, and then kept at ambient temperature for 24 hrs. The water part is drained out after phase separation and this process was repeated 4 times by changing the solution over the course of 2 days. The as-prepared aerogel displays a specific surface area of approximately 500 m^2/g and pore sizes ranging from a few nanometers to 50 nm, as identified in our prior study [23].

Synthesis of blended and hammermilled composites: Different compositions of blended-hammermilled composites were prepared by the varying different ratios of blended: hammermilled straw from (90:10 to 50:50). At first, the dried blended and hammermilled fibers are mixed in the desired ratio with 500 ml of DI water and made homogenous by using a mechanical agitator. Next, the mixture was poured into the paper-making setup, kept between metallic perforated sheets, and clamped using screws to maintain the thickness and avoid buckling. Finally, the as-prepared composites were kept in a preheated oven at 60°C at ambient pressure for drying.

Synthesis of cellulose-aerogel composite: Different wt % of cellulose-aerogel composites have been synthesized by varying aerogel concentration into the blended: hammermilled straw (90:10) mixture. The dried treated straw fibers were blended with 300 ml of DI water and then mixed with the required volume of aerogel using a mechanical agitator. The slurry was then poured into the paper-making setup. The composite-making and drying process is the same as the blended-hammermilled composite described above.

Physical Measurements: Fourier-transform infrared spectroscopy (FTIR-Agilent carry 560) was used to study the interfacial bonding and chemical bonding state of the composites. The scanning electron microscope (FIB-SEM, Carl Zeiss AURIGA Crossbeam) was used to study the microstructures of composites. The skeletal density (ρ_s) of the samples was measured using a pycnometer system (Micromeritics Accu-Pyc II 1340 Gas Pycnometer) which applies the gas displacement method to measure the volume and determine the density on a skeletal level. The bulk density of the composites is measured by equation (1).

$$\text{Density}\ (\rho) = \frac{\text{Mass}\ (m)}{\text{volume}\ (v)} \tag{1}$$

The porosity of the samples was calculated using equation 2:

$$\text{Porosity} = (1 - \frac{\rho_m}{\rho_s}) \tag{2}$$

The thermal conductivity of the composites is measured using the steady-state methodology and the heat flow meter -100 series (HFM-100, Thermtest), following ASTM C518 standard. Prior to each measurement, calibration was performed using the reference sample of NIST SRM 1450e with the similar thickness, which has a thermal conductivity of 32.5 mW/m.K. The flexural modulus measurements are conducted on specimens with dimensions of 130 mm x 25 mm x 6 mm, using a universal test system (Model SSTM-20KN from United Testing Systems). The thermal stability of the composites is examined using thermogravimetric analysis and differential scanning calorimetry (TGA/DSC) tests conducted with the TA Instrument DSC SDT Q600. During this characterization test, the composites samples are heat-treated in a nitrogen atmosphere (with a purge rate of 100 mL/minute) from room temperature to 550 °C at a heating rate of 20 °C/min. The fire retardancy of the composites is tested using the candle flame test method following the IEC 62441 standard. Before the test, it is necessary to ensure the flame reaches stable conditions. Throughout each test, the sample and the burner remain fixed at a constant distance. The mass loss of the samples during the test is recorded. For the hydrophobic wax coating, the composite samples are coated by immersing them for 20 mins in a dissolved wax solution in water. The coated samples are then dried in an oven at 60 °C. The water absorption capacity of the samples is evaluated by measuring the mass change after immersing the samples in water overnight at 20 °C. To investigate the recyclability of the composites, the prepared composite is blended with DI water using a blender. Then, the resulting slurry is poured into the paper-making setup, following the same composite-making and drying process described for the fresh composite above.

Acknowledgments

S.R. acknowledges the funding support on this work by the United States Department of Energy (DOE) Advanced Research Projects Agency-Energy (ARPA-E) award DE- AR0001771.

References

[1] O. Faruk, A. K. Bledzki, H.-P. Fink, M. Sain, Progress report on natural fiber reinforced composites, Macromol. Mater. Eng. 299 (2014) 9-26.

[2] H. Zhu, W. Luo, P. N. Ciesielski, Z. Fang, J. Y. Zhu, G. Henriksson, M. E. Himmel, L. Hu, Wood-derived materials for green electronics, biological devices, and energy applications, Chem. Rev. 116 (2016) 9305-9374.

[3] B. E. Dale, 'Greening' the chemical industry: research and development priorities for biobased industrial products, J. Chem. Technol. Biotechnol. 78 (2003)1093-1103.

[4] J. T. McNamara, J. L.W. Morgan, J. A Zimmer, A molecular description of cellulose biosynthesis, Annu Rev Biochem. 84 (2015) 895-921.

[5] K. Jaisamut, L. Paulová, P. Patáková, S. Kotúčová, M. Rychtera, Effect of sodium sulfite on acid pretreatment of wheat straw with respect to its final conversion to ethanol, Biomass & Bioenergy, 95 (2016) 1-7.

[6] F. Scrucca, C. Ingrao, C. Maalouf, T. Moussa, G. Polidori, A. Messineo, C. Arcidiacono, F. Asdrubali, Energy, and carbon footprint assessment of production of hemp hurds for application in building. Environ. Impact Assess. Rev. 84 (2020) 106417.

[7] G. Cheng, Y. Zhao, S. Pan, X. Wang, C. Dong, A comparative life cycle analysis of wheat straw utilization modes in China, Energy 194 (2020) 116914.

[8] S. H. Ghaffar, M. Fan, Revealing the morphology and chemical distribution of nodes in wheat straw. Biomass and Bioenergy, 77 (2015) 123-134.

[9] G. Tlaijia, F. Penneca, S. Ouldboukhitinea, M. Ibrahimc, P. Biwolea, Hygrothermal performance of multilayer straw walls in different climates. Constr. Build. Mater., 326 (2022) 126873.

[10] G. Dorez, A. Taguet, L. Ferry, J. M. Lopez-Cuesta, Thermal and fire behavior of natural fibers/PBS biocomposites. Polym. Degrad. Stab. 98 (2013) 87-95.

[11] L. Costes, F. Laoutid, S. Brohez, P. Dubois, Bio-based flame retardants: When nature meets fire protection, Mater. Sci. Eng., R. 117 (2017) 1-25.

[12] Z. K. Du, G.W. Wang, S. X. Gao and Z. Y. Wang, Aryl organophosphate flame retardants induced cardiotoxicity during zebrafish embryogenesis: by disturbing expression of the transcriptional regulators, Aquat. Toxicol. 161 (2015) 25-32.

[13] R. Hou, Y. P. Xu, Z. J. Wang, Review of OPFRs in animals and humans: Absorption, bioaccumulation, metabolism, and internal exposure research, Chemosphere. 153 (2016) 78-90.

[14] A. K. Greaves, R. J. Letcher, Comparative body compartment composition and *In Ovo* transfer of organophosphate flame retardants in north american great lakes herring gulls. Environ. Sci. Technol. 48 (2014) 7942-7950.

[15] Anon. flame retardants: European union risk assessments update. Plast. Addit. Compd. 6 (2004) 26-29.

[16] R. C. Hale, M. J. La Guardia, E. Harvey, M. O. Gaylor, T. M. Mainor, Brominated flame-retardant concentrations and trends in abiotic media, Chemosphere 64 (2006)181-186.

[17] M. Farooq, M. H. Sipponen, A. Seppalä, M. Ö. sterberg, Eco-friendly Flame-retardant cellulose nanofibril aerogels by incorporating sodium bicarbonate. ACS Appl. Mater. Interfaces. 10 (2018) 27407-27415.

[18] P. S. Jadhav, A. Sarkar, S. Pasupathy, S. Ren, Biogenic straw aerogel thermal insulation materials, Adv. Eng. Mater. 25 (2023) 2300037.

[19] E. Mazzon, A. Habas-Ulloa, J. P. Habas, Lightweight rigid foams from highly reactive epoxy resins derived from vegetable oil for automotive applications, Eur. Polym. J. 68 (2015) 546-557.

[20] S. Girish, K. Devendra, K.N. Bharath, Effect of Sodium bicarbonate on Fire behaviour of filled Glass Reinforced Epoxy Composites, IOP Conf. Ser. Mater. Sci. Eng.149 (2016) 012120.

[21] Q. Zhen, T. Zhou, Y. Wang, X. Cao, S. Wu, M. Zhao, H. Wang, M. Xu, B. Zheng, J. Zheng, X. Guan, Pretreatment of wheat straw leads to structural changes and improved enzymatic hydrolysis, Sci. Rep**.** 8 (2018) 1321.

[22] S. Gorgieva, U. Jancˇicˇ, S. Hribernik, D. Fakin, K. S. Kleinschek, S. Medved, T. Fakin, M. Bozˇic, Processing and functional assessment of anisotropic cellulose nanofibril/Alolt/sodium silicate: based aerogels as flame retardant thermal insulators, Cellulose, 27 (2020)1661-1683.

[23] L. An, M. Di Luigi, D. Petit, Y. Hu, Y. Chen, J.N. Armstrong, Y.C. Li, and S. Ren, Nanoengineering porous silica for thermal management. ACS Appl. Nano Mater. 5 (2022) 2655-2663.

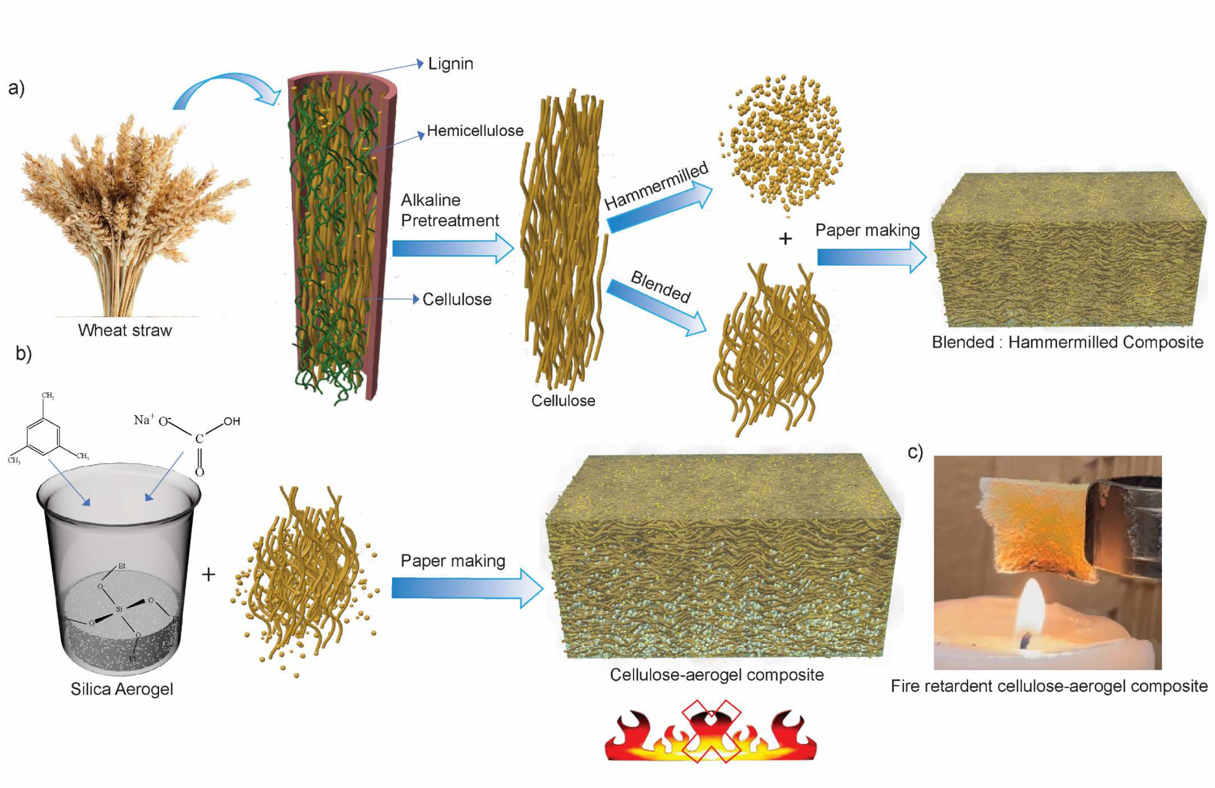

Fig. 1 Schematic diagram of alkaline treatment of wheat straw and fabrication of blended: hammermilled composite, b) Synthesis of fire-retardant cellulose-aerogel composite, c) Image of the fire retardant cellulose-aerogel composite.

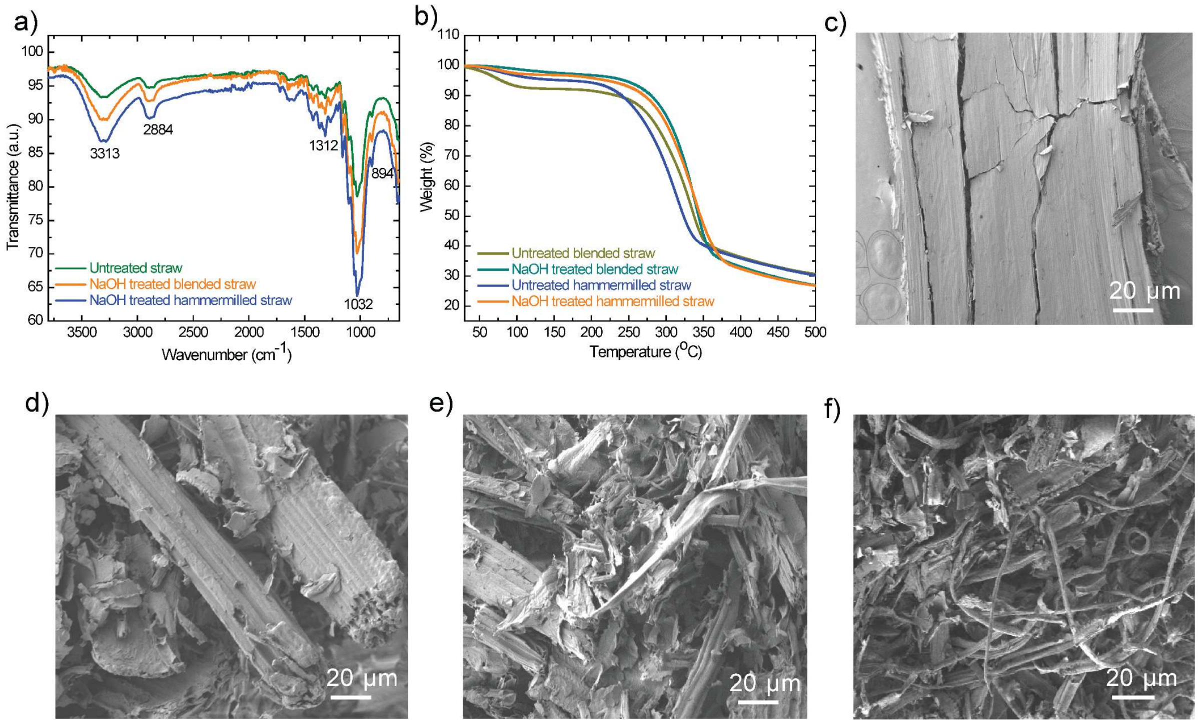

Fig. 2 a) FTIR spectra of untreated and NaOH treated wheat straw, b) TGA curves of untreated and NaOH treated wheat straw, c) SEM image of raw wheat straw, d) SEM image of raw hammermilled straw, e) SEM image of NaOH treated blended straw, f) SEM image of NaOH treated hammermilled straw.

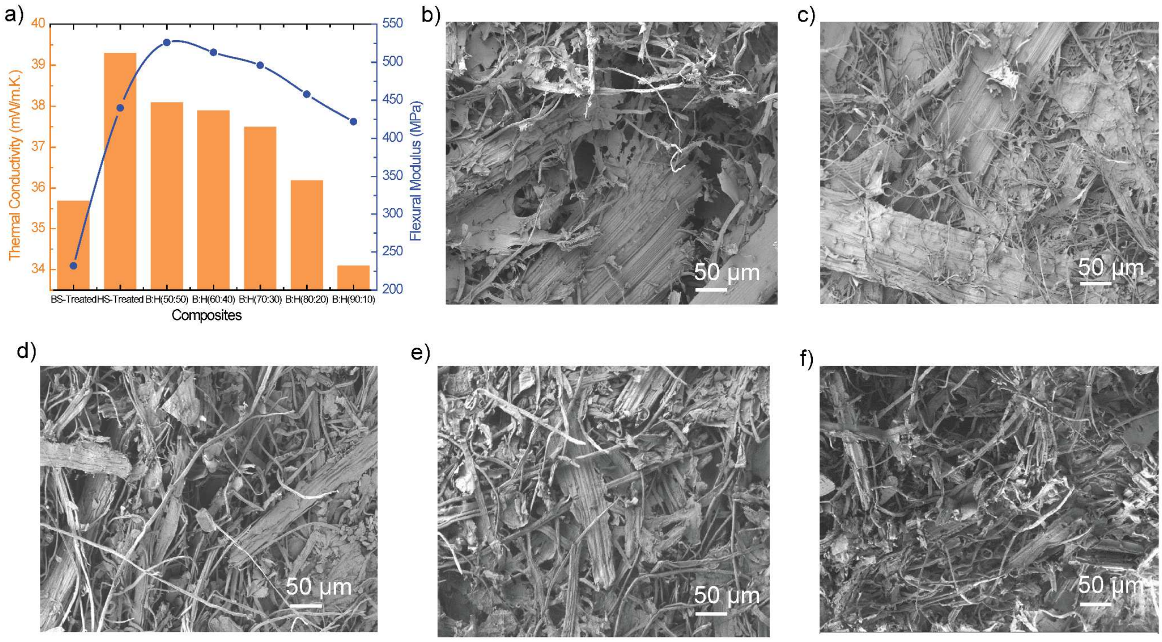

Fig. 3 a) Thermal conductivity vs flexural modulus plot of blended: hammermilled straw composites, b) SEM image of B: H (90:10) composite, c) SEM image of B: H (80:20) composite, d) SEM image of B: H (70:30) composite, e) SEM image of B: H (60:40) composite, f) SEM image of B: H (50:50) composite.

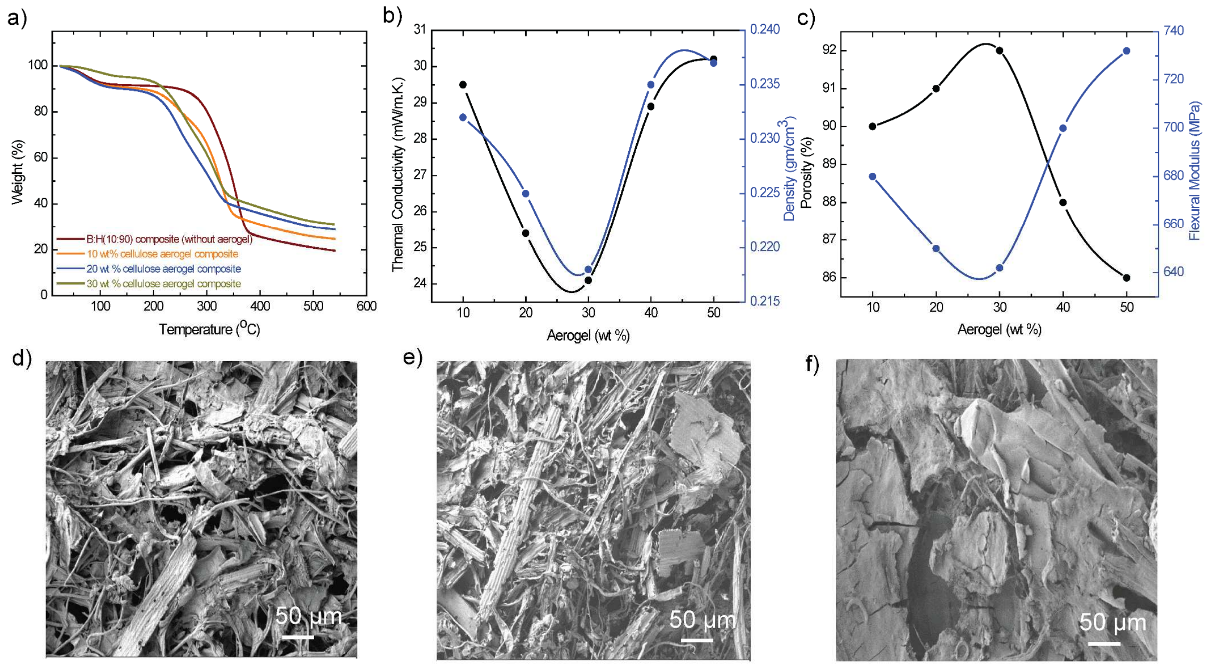

Fig. 4 a) TGA curves of different wt % of aerogel-cellulose composite, b) Thermal conductivity vs aerogel concentration variation plot of cellulose-aerogel composite, c) Flexural modulus vs aerogel (wt%) plot of cellulose-aerogel composite, d), e), and f), SEM images of 10 wt %, 30 wt % and 50 wt % cellulose -aerogel composite respectively.

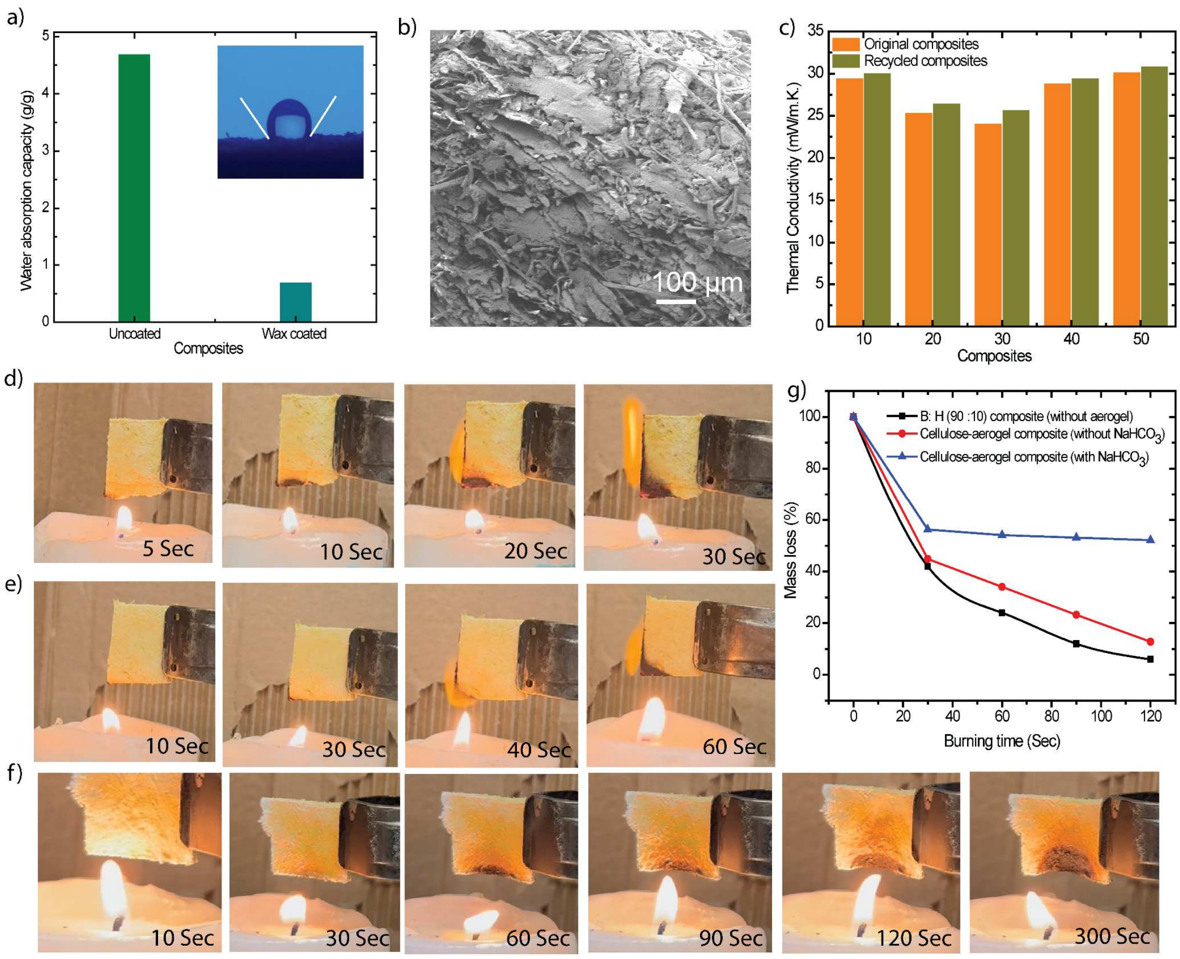

Fig. 5 a) Change in water absorption capacity of wax coated and uncoated cellulose-aerogel composite; (inset) water contact angle for the wax-coated composite, b) SEM image of wax coated composite, c) Reusability test of cellulose-aerogel composite, d), e), f) Flame retardancy test of without aerogel composites, TEOS based cellulose aerogel composites (without sodium bicarbonate) and sodium bicarbonate containing TEOS based cellulose aerogel composite respectively, g) Mass loss vs burning time plot of without aerogel composites, TEOS based cellulose aerogel composites and sodium bicarbonate containing TEOS based cellulose aerogel composite.

<u>Graphical Abstract</u>

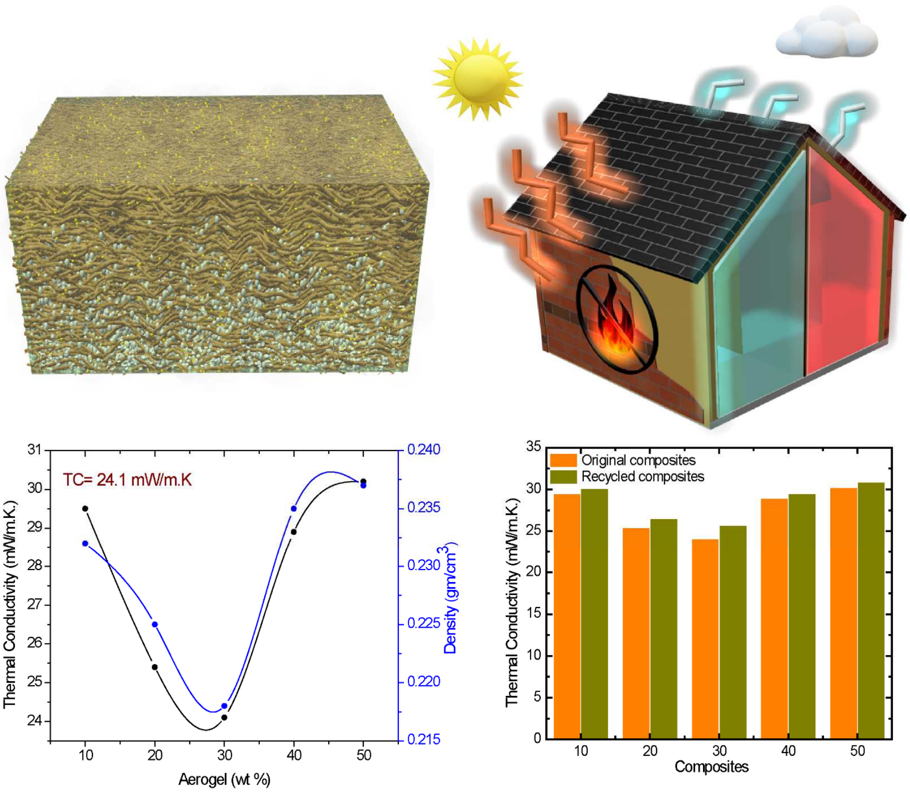

Graphical Abstract